Titan Interaction with Saturn's Magnetosphere: Voyager 1 Results Revisited

E. C. Sittler Jr.[1], R. E. Hartle[1], A. F. Viñas[1] , R. E. Johnson[2], H. T. Smith[2] and I. Mueller-Wodard[3]

1. NASA/Goddard Space Flight Center, Greenbelt, MD, 20771, USA, Email: edward.c.sittler@nasa.gov, richard.e.hartle@nasa.gov, adolfo.f.vinas@nasa.gov
2. University of Virginia, Engineering Physics, Thornton Hall Room B103, Charlottesville, VA, 22904, USA, Email: rej@virginia.edu
3. Imperial College, London, UK, Email: i.mueller-wodarg@imperial.ac.uk

We investigate the details of Titan's interaction with Saturn's magnetosphere, which includes formation and location of an ionopause, mass loading via ion pickup and the effects of finite gyroradii . We present new interpretations of the Voyager 1 plasma instrument measurements, not addressed by Hartle et al. (1982). Pickup ions H^+ and H_2^+ dominate the outermost region from the Titan's ionopause, followed by CH_4^+ at intermediate distances and N_2^+ just outside the exobase. Mass loading and slowing down of the ambient plasma increase as the pickup ion mass increases with decreasing distance from Titan's ionosphere. H_2^+ and CH_4^+ are ions in the exosphere at the time of the Voyager I flyby. Therefore, Titan could be an important source of carbon to Saturn's magnetosphere. Finite gyroradius effects are identified in the plasma interaction with Titan's atmosphere, which results in an asymmetric removal of ambient plasma from Titan's ion exosphere region. The finite gyro-radius effects also show that the hot keV ion component for the ambient plasma as observed by plasma instrument is a heavy ion such as N^+. A minimum ionopause altitude of 4800 km is estimated by a new approach using mass loading.

1.0 Introduction

A new picture of the interaction of Saturn's rotating magnetospheric plasma with Titan's atmosphere emerged from measurements made by instruments onboard Voyager 1 as it flew by Titan on November 12, 1980. Since then a number of the atmosphere, ionosphere and interaction models (Yung et al., 1984; Yung, 1987; Toublanc et al., 1995; Keller et al., 1998) have been developed that encourage further analysis of this data. Consequently, we extend our earlier interpretation of the plasma measurements in an attempt to account for some of the new information embodied in the recent models.

Voyager 1 plasma and field instruments detected a complex interaction with Saturn's outer magnetosphere (Bridge et al. (1981) and Ness et al. (1981)). These initial results were followed by the more comprehensive analysis (Hartle et al. (1982), Ness et al. (1982) and Neubauer et al. (1984)). The upstream parameters are summarized in Table 1. They showed that the sonic Mach number was less than 1, no shock was detected and the magnetometer did not detect an internal magnetic field. The rotating plasma is composed of H^+ and N^+, having densities of 0.1 cm^{-3} and 0.2 cm^{-3} and temperatures of 210 eV and

2.9 keV, respectively. The electron's density is 0.3 cm^{-3} with a temperature of 200 eV. These constituents yield a high kinetic pressure (due primarily to the hot N^+) relative to that of the observed 5 nT magnetic field, resulting in a plasma beta of about 11. Hartle et al. (1982), showed that ambient N^+ had gyroradii $r_g > 5000$ km, which are larger than the physical dimensions of Titan, making finite gyro-radius effects an essential feature of the interaction. The analysis by Hartle et al. (1982) demonstrated that the inbound pass was very complex and that pickup ions had been observed. This result was supported by the enhanced levels of wave emissions observed by the Plasma Wave System (PWS) instrument during the inbound approach (Gurnett et al., 1981; Gurnett et al., 1982). In the analysis by Hartle et al. (1982), hereafter referred to as Paper I, they modeled the pickup ions by using a ring distribution, which then had to be convoluted with the Plasma Science (PLS) instrument's response (see Bridge et al., 1977 for a description of the instrument). In order to simulate the pickup process they used an exosphere model (Hartle et al., 1971, 1973a,b) composed of H and N_2, the constituents known to exist in the exosphere at the time. With regard to the finite gyro-radius aspects of the interaction, one would surmise that the use of MHD codes to model the interaction may not apply, although the MHD model by Cravens et al. (1998) was developed later on to model the interaction. This work was then followed by that of Brecht et al. (2000) who developed a 3D hybrid calculation of the interaction which did model the finite gyro-radius aspects of the interaction. This model only included a single ion component, used an ad hoc description of the pickup ion process and its cell size was sufficiently large that it could not resolve the ionopause boundary.

For this paper we revisit the original analysis of Paper I and provide new insights about the nature of the interaction. In addition to H and N_2, we have added H_2, CH_4 and exothermic nitrogen atoms, N*, to our exospheric model. We then use this model to compute mass loading of the plasma by pickup ions, which are formed primarily by photoionization, electron impact ionization and charge-exchangeof the neutral exosphere.

2.0 Voyager 1 Encounter with Titan Revisited

2.1 Encounter Geometry and Inferred Model of Interaction

In Figure 1 we show the Voyager 1 flyby geometry, along with the view axes of the A, B, C and D cups of the plasma instrument during the encounter period. Paper I located the points numbered 1 to 8 along the spacecraft trajectory, where the PLS ion spectra were analyzed to characterize Titan's interaction with Saturn's magnetosphere. The sensor alignment is such that the D cup is pointing directly into the corotation direction, the C cup has partial alignment along the corotation direction, while the A and B cups look at right angles to the corotation direction. During Voyager I, the ambient plasma was moving about 20 degrees from the corotation direction, toward Saturn at a mean speed of 120 km/s (velocity range of 80-150 km s^{-1}, Paper I). The maximum flux of the pickup ions comes from this flow direction and gives the largest signal in the D cup. Titan was near local noon relative to Saturn and thus near it's magnetopause boundary.

Some of the inferred properties of Titan's interaction with Saturn's magnetosphere, as envisioned in Paper I, are shown in Figure 1, where the estimated location of the ionopause, R_{ion} ~ 4400 km and the exobase, R_{exo} ~ 4000 km are indicated. The Cassini spacecraft, for its planned 40 plus Titan encounters, will come as close as 1000 km or less of Titan's surface. The figure also shows a deflection of the wake by about 20° from the corotational direction, which was interpreted in Paper I to be caused by an inward deflection of the magnetopause due to an increase in solar wind pressure and Titan's close proximity to the magnetopause. The figure shows the cycloidal trajectory of pickup hydrogen ions observed during the spacecraft's inbound leg of Titan's flyby.

2.2 Analysis of Plasma Data: New Results

In Figure 2 we show, as done in Paper I, six of the eight PLS ion spectra analyzed for study of the Titan interaction (spectra 5 and 6 in the ionotail are not included for brevity). Spectra 1 and 8 were measured when the spacecraft was far from the interaction region and showed the presence of very hot ambient magnetospheric plasma described above. In Table 2, we show estimated ion gyro-radii for the ambient plasma, spectrum 1, and possible pickup ion components for spectra 2, 3 and 4. The table shows gyro-radii for ambient protons of ~ 400 km, while that for N^+ of ~ 5600 km, the latter being greater than the diameter of Titan. Considering Figure 1 and spectrum 2 in Figure 2, when the spacecraft is ~ 5500 km from the center of the deflected wake, attenuation of ambient nitrogen ions, residing toward keV energies, is apparent. The ambient protons at lower energies are essentially unaffected Also, there is the possible presence of pickup ions in the D cup at energies extending up to 500-1000 eV. In spectrum 3 the ambient nitrogen ions are essentially removed and the ambient protons are also showing attenuation toward higher energies. The dominant feature for this spectrum is the presence of a pickup ion component with energy below a few hundred eV. The magnetometer data indicates that spectrum 4 is just outside the wake region. In spectrum 7, when the spacecraft exits the wake, only ambient protons appear and in spectrum 8 both ambient protons and nitrogen ions have completely recovered. Overall inspection of these figures indicates a preference for the ambient nitrogen ions to be removed during the inbound pass relative to that on the outbound pass. This result is interpreted in terms of finite gyro-radius effects that occur when the magnetosphere plasma interacts with Titan's atmosphere. Both the spacecraft position of spectrum 2 and the gyroradii of the ambient nitrogen ions are about the distance Voyager 1 is from the wake region. Thus, upstream N^+ ions, whose guiding center trajectories pass between the spacecraft and the wake, will have a high probability of gyrating into Titan's atmosphere and be lost from the plasma flow as suggested in spectrum 2. On the other hand, the ambient protons, having gyroradii of only about 400 km, will not encounter Titan's atmosphere and thus show little attenuation at spectrum 2. Spectrum 3 is only about 1000-2000 km from the wake boundary. Consequently, if ambient N^+ ions are to be observed in any of the Faraday cups, their guiding center trajectories would be inside the wake. In this case, ambient N^+ has a high likelihood of encountering Titan's upper atmosphere and disappear from the plasma flow, as observed. The same can be said for spectrum 7 during the outbound pass. The absence of ambient nitrogen in spectrum 7 is consistent with their large gyroradii and closeness of the spacecraft to the wake. While the ambient protons with their smaller gyroradii show

nearly full recovery. In order for the ions to be observed by cups C and D, their guiding centers must be further away from Titan with respect to the spacecraft to increase their probability of not encountering Titan's upper atmosphere. By spectrum 8, the spacecraft is ~ 3000 km from the wake. Since the guiding centers of these ions are on the Saturn side of the spacecraft, they do not encounter Titan's atmosphere and as observed have no attenuation. As can be inferred from Figure 1, ions entering cups A and B, can have their guiding centers further away from Titan during the inbound pass, relative to that required for cups C and D. There is evidence, especially for cup A, which looks furthest from the corotation direction than the other three sensors, that ambient nitrogen ions are present in spectrum 2 as expected. Cup D in Figure 2 does show some signal up to 5 keV (weaker at lower energies than spectrum 1), but this could be due to a heavy pickup ion component forming further upstream before mass loading has taken effect (i.e., r_g ~ 7300 km). Ions observed in spectrum 7 by A and B cups must have their guiding centers shifted toward Titan with respect to ion trajectories sensed by cups C and D. Therefore, the guiding centers of ambient protons must be no closer than ~ 400 km from the upper atmosphere of Titan (i.e., above the exobase). The location of the inferred boundary of the wake, as shown in Figure 1, is consistent with this interpretation. Altogether, it should be clear from the above discussion, that finite gyroradius effects do play an important role in the physics of Titan's interaction with Saturn's magnetosphere. A similar effect as described above was suggested by the hybrid calculations of Brecht et al. (2000), but they gave no reason for the effect. The finite gyro-radius effects reported here, also clearly show that the hot keV ion component of the ambient plasma is a heavy ion such as N^+.

Returning to spectrum 2, the location of the high energy edge of the pickup ion peak will be equivalent to twice the flow speed of the plasma if the ions are described by a ring distribution. In Table 2 we indicate our estimated drift speeds of the plasma for an assumed composition of the pickup ions. If protons, the inferred drift speed of 175 km/s exceeds our upper estimate of 150 km/s for the flow speed of the ambient plasma. In the case of N^+ (equivalent to CH_4^+) the drift speed is ~ 50 km/s, which is below our lower range of 80 km/s for the flow speed of the ambient plasma. But it would be consistent with some mass loading of the plasma by the pickup ions. If the ion is N_2^+, the drift speed is ~ 33 km/s. Note that the gyroradii of the pickup ions are 350 km < r_g < 1800 km, considerably less than the gyroradii of ambient nitrogen ions r_g ~ 5600 km. For spectrum 3, where the pickup ions are confined below a few hundred eV, the estimated drift speeds are ~ 85 km/s, 23 km/s and 16 km/s for H^+, N^+ (CH_4^+) and N_2^+, respectively. At this point, considerable mass loading of the plasma has occurred. We also see a further decrease in the gyroradii of the pickup ions, where 170 km < r_g < 900 km. Finally, in spectrum 4, the spectral peak is confined below the low energy cut-off of the PLS instrument, 10 eV, and the inferred flow speeds are 60 km/s, 10 km/s and 5 km/s for H^+, N^+ (CH_4^+) and N_2^+, respectively. Here, the plasma flow is very close to the wake boundary and severe mass loading of the plasma has occurred and is probably composed of N_2^+ ions. At this point, the flow is more fluid like, and the gyroradii are 120 km < r_g < 280 km. In conclusion, we can say, further from the wake, finite gyro-radii effects are dominant, while near the ionopause boundary, the flow becomes more fluid like. Therefore, future models must consider these issues. The numerous close encounters of

the Cassini spacecraft with Titan will allow us to constrain models of the interaction over a wide range of encounters and Titan interaction geometries, which could include Titan's interactions within Saturn's magnetosheath or the solar wind.

3.0 Titan's Exosphere

3.1 General Exosphere Properties

We extend the exosphere model in Paper I, which included H and N_2, constituents observed at the time. Atmosphere models by Keller et al. (1998), Yung (1987), Yung et al. (1984) and Toublanc et al. (1995) predicted significant quantities of H_2 and CH_4 in the exosphere. We include these species and added the ejection of suprathermal nitrogen atoms, due to electron and photon dissociation of N_2 (Strobel and Shemansky, 1982; Ip, 1992; Strobel et al. 1992) and sputtering due magnetospheric ion impact (Shemantovich 1998,1999; Shemantovich et al. 2001). The results are shown in Figure 3 for a spherically symmetric model of the exosphere. As can be seen H_2, H and N* dominate far from Titan with H_2 an order of magnitude larger than H, while H is two orders of magnitude larger than N*. Because methane is lighter than N_2 it will dominate for heights greater than a few hundred kilometers above the exobase at r ~ 4000 km, until a height ~ 1500 km when H_2 starts to dominate. Note that the mass density of CH_4 will dominate over that of H_2 for heights up to 2500 km. This will be important when considering mass loading calculations. Finally, when within a few scale heights of the exobase, N_2 will dominate over everything else, especially its mass density.

4.0 **Mass Loading Calculations: Ionopause Location?**

Using the exosphere model described above, we compute the effects of mass loading on the flow of the ambient plasma due to pickup ions as in Paper I. The ionopause altitude is estimated to be the point above the ionosphere where the mass loaded plasma velocity vanishes. The pickup ions are formed by ionizing the neutral exosphere constituents, which include H_2, N*, and CH_4 in addition to H and N_2 used in Paper I. We include photoionization, electron impact ionization and charge exchange reactions in our model calculations. The cross-sections and reaction rates are summarized in Table 3. The plasma velocity, V, along a streamline, s, is obtained by solving the mass conservation and momentum equations

$$\frac{\partial \rho V}{\partial s} = \sum_j m_j P_j - \sum_k m_k L_k \qquad (1a) \qquad\qquad \rho V \frac{\partial V}{\partial s} = -2V \sum_j m_j P_j \qquad (1b)$$

where,

$$\rho = \sum_j m_j N_j \qquad (2a) \qquad\qquad V = \sum_j m_j N_j V_j / \sum_j m_j N_j \qquad (2b)$$

The total mass density, ρ, and the bulk velocity component, V, along the streamline s are obtained by summing over all ion species whose components include the j-th ion mass, m_j, ion density N_j, and ion velocity, V_j,. P_j is the total volume production rate for the j-th

ion and L_k is the charge-exchange volume loss rate of the kth ion. The momentum equation (1b) has been simplified by only including the impulse force due ion pickup, while ignoring the pressure gradient force, $\partial p/\partial s$, and the magnetic force, $\mathbf{j}x\mathbf{B}$. These calculations, which only include mass loading effects and are intrinsically 1D in character, tend to over-estimate the ionopause height, while the missing horizontal flow component will tend to move our predicted ionopause position inward. The Venus results by Hartle et al. (1980) would expect this boundary to be further outward because of the expected pile up of plasma and magnetic field above the ionopause which can cause the total pressure gradient force (particle plus field) to point upstream in the same direction as the impulse force. The Cravens et al. (1998) MHD results would argue that the total plasma pressure would be almost a constant above the boundary and have little effect on our predicted ionopause location. The numerous Cassini encounters with Titan is expected to identify the differences between Venus and Titan.

In Figure 1, the geometry used for our calculations is shown for a fluid element moving past Titan with impact parameter b. In these calculations we ignore deflections and compressions/expansions of the fluid element as it moves past Titan. In the case of zero impact parameter, b=0, the fluid element moves towards Titan along the axis parallel to the flow, through the origin, at 20° to the x-axis. When mass loading becomes large, the plasma stops at a boundary we identify as the "ionopause". In Figure 4 we show the reduction in flow speed along a streamline with impact parameter b = 0, where considerable deceleration occurs between 5000 km and 6000 km. In Paper I, the "ionopause" was estimated to be at ~ 4400 km. In the case b = 0, we estimate the "ionopause" location to be ~ 4800 km. The addition of methane, which extends to larger distances than N_2, may account for some of the difference between the two calculations. We note that the ionopause altitude estimated in paper I was where the ion-neutral mean free path equaled the horizontal scale height. Below such an altitude, the ions formed would tend to be tied to the neutral atmosphere and behave more like ionospheric ions.

At an impact parameter of b = 6000 km, the flow speed decreases considerably before it asymptotes to ~ 60 km/s as the plasma moves past Titan. This speed is lower than expected for H^+ in Table 1. Considering the flow to be 20 degrees or more from the x-axes, as shown in Figure 1, and using the values in Table 1, we would argue that this calculation may pertain to spectrum 2, where the pickup ion might be CH_4^+. We note that the gyroradius of CH_4^+ at its birthplace upstream is greater than the scale height of its source (not true for H and H_2). In this case, the observed cutoff energy is expected to be less than that corresponding to 2x the drift speed of the ambient plasma (Hartle and Sittler, 2004). Consequently, the 47 km/s at for CH_4^+ in Table 1 is a lower limit. In the case of b = 5558 km, the flow speed decreases to an asymptotic value ~ 5 km/s as the fluid element moves past Titan. If the "ionopause" is ~ 4800 km, spectrum 4 is consistent with this calculation for which Table 2 shows the drift speed to be ~ 5 km/s for pickup N_2^+. For lower impact parameters the flow decreases rapidly. Under these circumstances, the flow must be moving tangent to the "ionopause" boundary. The general features of this interpretation are supported by our plot of the ion mass density along a streamline (i.e., for cases b = 0, 5558 km and 6000 km) for the various pickup ion species. Spectrum 3 would be intermediate to cases b = 6000 km and 5558 km.

Our calculations have ignored the effects of the plasma pressure gradient force and the magnetic force which may tend to cancel each other out. Since the above calculation using (Eqs. 1 a, b) is a fluid approximation, the impulse force assumes that the ions are instantaneously picked up at the ambient drift speed. This tends to overestimate the impulse force due to finite gyroradius. The problem arises because heavy ions like N_2^+ have gyroradii that are much larger than the scale height of the source gas. Such ions born in the last scale height or two above the ionopause may never attain the ambient drift speed over the acceleration region studied, thereby leading to an overestimate of the impulse force. Consequently, finite gyroradius corrections would put the ionopause below 4800 km. However, the altitude where ion neutral drag stops the flow would determine the ultimate limit.

REFERENCES

1. Albritton, D. L., Ion-neutral reaction-rate constants measured in flow reactors through 1977, *At. Nucl. Data Tables, 22*, 1-101, 1978.
2. Basu et al., Linear transport theory of auroral proton precipitation: A comparison with observations, *J. Geophys. Res.*, **92**, 5920-5932, 1987.
3. Brecht, S. H., Luhmann J. G. and Larson D. J., Simulation of the Saturnian magnetospheric interaction with Titan, *J. Geophys. Res.*, **105**, 13,119-13,130, 2000.
4. Bridge, H.S., J.W. Belcher, R.J. Butler, A.J. Lazarus, A.M. Mavretic, J.D. Sullivan, G.L. Siscoe and V.M. Vasyliunas, The plasma experiemtn on the 1977 Voyager Mission, *Space Sci. Rev.,* **21**, 259, 1977.
5. Bridge, H. S., et al., Plasma observations near Saturn: Initial results from Voyager 1, *Science*, **212**, 217, 1981.
6. Cravens, T. E., C. J. Lindgren and S. A. Ledvina, A two-dimensional multi-fluid MHD model of Titan's plasma environment, *Planet. Space Sci.*, **46**, 1193-1205, 1998.
7. Freysinger, W. et al., "Charge-transfer reaction of $^{14,15}N^+(^3P_J)+N_2(^1\Sigma_g^+)$ from thermal to 100 eV Crossed-beam and scattering-cell guided-ion beam experiments", J. Chem. Phys. 101, 3688-3695, 1994.
8. Hartle, R. E., Model for rotating and non-uniform planetary exospheres, *The Physics of Fluids*, **14**, 2592, 1971.
9. Hartle, R. E., Density and temperature distributions in non-uniform rotating planetary exospheres with application to Earth, *Planet. Space Sci.*, **21**, 2123, 1973.
10. Hartle, R. E., K. W. Ogilvie and C. S. Wu, Neutral and ion-exospheres in the solar wind with application to Mercury, *Planet. Space Sci.*, **21**, 2181, 1973.
11. Hartle, R. E., H. A. Taylor, Jr., S. J. Bauer, L. H. Brace, C. T. Russel and R. E. Daniell, J.r, Dynamical response of the dayside ionosphere of Venus to the solar wind, *J. Geophys. Res.,* **85**, 1980.

12. Hartle, R. E., E.C. Sittler Jr., K. W. Ogilvie, J. D. Scudder, A.J. Lazarus and S. K. Atreya, Titan's ion exosphere observed from Voyager 1, *J. Geophys. Res.*, **87**, 1383, 1982.
13. Hartle, R. E. and E. C. Sittler, Jr., Pickup ion velocity distributions at Titan: Effects of spatial gradients, *Eos. Trans.* AGU, **85(17)**, Joint Assembly Suppl., Abstract, P33D-04, 2004.
14. Huebner, W. F. and P. T. Giguere, A model of comet comae,II, Effects of solar photodissociation ionization, *Astrophys. J.*, **238**, 753, 1980.
15. Huntress, W. T., Jr., Laboratory studies of bimolecular reactions of positive ions in interstellar clouds, in comets, and in planetary atmospheres of reducing composition, *Astrophys. J. Suppl. Ser.*, **33**, 495-514, 1977.
16. Ip, W., -H., The nitrogen tori of Titan and Triton, *Adv. Space Res.*, **12**, (8)73, 1992.
17. Keller, C. N., V. G. Anicich and T. E. Cravens, Model of Titan's ionosphere with detailed hydrocarbon ion chemistry, *Planet. Space Sci.*, **46**, 1157-1174, 1998.
18. Koopman, D. W., Charge exchange in CH_4 and NH_3*, *J. Chem. Phys.*, **49**, 5203, 1968.
19. Lo, H. H., et al., Electron capture and loss collisions of heavy ions with atomic oxygen, *Phys. Rev.*, **A4**, 1462-1476, 1971.
20. Lotz, W., Electron-impact ionization cross-sections and ionization rate coefficients for atoms and ions, *Astrophys. J. Suppl. Ser.*, **14**, 207-238, 1967.
21. Massay, H. S. and H. B. Gilbody, Electronic and ionic impact phenomena, in *Recombination and Fast Collisions of Heavy Particles*, vol. IV, Oxford University Press New York, pp. 2782, 1974.
22. Neubauer, F.M., D.A. Gurnett, J.D. Scudder, and R.E. Hartle, Titan's magnetospheric interaction, in *Saturn,* eds. T. Gehrels and M.S. Matthews, Univ. of Arizona Press, Tucson, 571, 1984.
23. Ness, N. F., M. H. Acuna, R. P. Lepping, J. E. P. Connerney, K. W. Behannon, L. F. Burlaga, F. M. Neubauer, Magnetic field studies by Voyager 1: Preliminary results at Saturn, *Science*, **212**, 211, 1981.
24. Ness, N. F., M. H. Acuna, K. W. Behannon, and F. M. Neubauer, The induced magnetosphere of Titan, *J. Geophys. Res.*, **87**, 1369-1381, 1982.
25. Newman, J. H., J. D. Cogan, D. L. Ziegler, D. E. Nitz, R. D. Rundel, K. A. Smith and R. F. Stebbings, Charge transfer in H^+-H and H^+ - D collisions within the energy range 0.1 – 150 eV, *Phys. Rev. A.*, **25**, 2976, 1982.
26. Phaneuf, R.A., et al., Single-electron capture by multiply charge ions of carbon, nitrogen and oxygen in atomic and molecular hydrogen, *Phys. Rev.*, **A4**, 534-545, 1978.
27. Phelps, A. V., Cross sections and swarm coefficients for nitrogen ions and neutrals in N_2 and Argon ions and neutrals in Ar for energies from 0.1 eV to 10 eV, *J. Phys. Chem.Ref. Data*, **20**, 557-573, 1991.
28. Rapp, D. and P. Englander-Golden, Total cross sections for ionization and attachment in gases by electron impact. I. Positive ionization, *J. Chem. Phys.*, **43**, 1464, 1965.
29. Rees, M. H., "Physics and chemistry of the upper atmosphere", Cambridge Univ. Press, 1989.

30. Rudd, M. E., Y.-K., D. H. Madison and J. W. Gallagher, Electron production in proton collisions: total cross sections, *Rev. Mod. Phys., Vol. 57, No. 4,* 965, 1985.
31. Shemantovich, V.I., Kinetic modeling of suprathermal nitrogen atoms in the Titan's atmosphere: I. Sources, *Solar System Research,* **32**, 384, 1998.
32. Shemantovich, V.I., Kinetic modeling of suprathermal nitrogen atoms in the Titan's atmosphere: II. Escape flux due to dissociation processes, *Solar System Research,* **33**, 32, 1999.
33. Shematovich, V.I., C. Tully and R.E. Johnson, Suprathermal nitrogen atoms and molecules in Titan's corona, *Adv. Space Res.,* **27**, 1875-1880, 2001.
34. Sittler, E. C., Jr. and R. E. Hartle, Triton's ionospheric source: Electron Precipitation or Photoionization, *J. Geophys. Res.*, **101**, 10,863, 1996.
35. Sittler, E. C., Jr., R.E. Johnson, H.T. Smith, J.D. Richardson, S. Jurac, M. Moore, J.F. Cooper, B. H. Mauk, M. Michael, C. Paranicas, T. P. Armstrong, and B. Tsurutani, Energetic Nitrogen Ions within the Inner Magnetosphere of Saturn, *J. Geophys. Res.*, submitted, 2004a.
36. Sittler, E.C., Jr.,R.E. Johnson, S. Jurac, J.D. Richardson, M. McGrath ,F. Crary, D. Young and J.E. Nordholt, Pickup ions at Dione and Enceladus: Cassini Plasma Spectrometer Simulations, *J. Geophys. Res.,* **109**, A01214, 2004b.
37. Strobel, D.F. and D.E. Shemansky, EUV emission from Titan's upper atmosphere: Voyager 1 encounter, *J. Geophys. Res.*, **87**, 1361-1368, 1982.
38. Strobel, D.F., M.E. Summers and X. Zhu, Titan's upper atmosphere: Structure and ultraviolet emissions, *Icarus,* **100**, 512, 1992.
39. Tawara, H., Cross sections for charge transfer of hydrogen beams in gases and vapors in the energy range 10 eV – 10 keV, *At. Data Nucl. Data Tables,* **22**, 491-525, 1978.
40. Tawara, H. et al, "Cross sections for electron capture and loss by positive ions in collisions with atomic and molecular Hydrogen", Atomic Data and nuclear Data Tables 32, 235-303,1985. .
41. Toublanc, D., J. P. Parisot, D. Gautier, F. Raulin and C. P. McKay, Photochemical modeling of Titan's atmosphere, *Icarus*, **113**, 2, 1995.
42. Yung, Y. L., An update of nitrile photochemistry on Titan, *Icarus*, **72**, 468, 1987.
43. Yung, Y. L., M. Allen and J. P. Pinto, Photochemistry of the atmosphere of Titan: Comparison between model and observations, *Astrophys. J. Suppl.*, **55**, 465, 1984.

Table 1. Plasma Upstream Properties: Voyager 1 Titan Flyby[1]

Parameter	Value
Magnetic Field B	5 nT
Flow Speed V	80-150 km/s
Proton Density n_p	0.1 cm^{-3}
Nitrogen Ion Density n_{N+}	0.2 cm^{-3}
Electron Temperature T_e	200 eV
Proton Temperature T_p	210 eV
N^+ Temperature T_{N+}	2.9 keV
Total Plasma Pressure p	10^{-9} dyne/cm^2
Plasma β	11
Alfven Speed V_A	64 km/s
Sound Speed V_S	210 km/s
Alfven Mach Number $M_A=V/V_A$	1.9
Sonic Mach Number $M_S = V/V_S$	0.57

1. Parameters derived from Hartle et al. (1982) and Neubauer et al. (1984)

Table 2. Ion Drift Speeds and Gyro-Radii at Titan

Spectrum #	Parameter	H^+	N^+	N_2^+
1	Thermal Speed	200 km/s	200 km/s	140.0 km/s
1	Gyro-Radius	400 km	5600 km	7840 km
2	Drift Speed	175 km/s	47 km/s	33 km/s
2	Gyro-Radius	350 km	1316 km	1848 km
3	Drift Speed	85 km/s	23 km/s	16 km/s
3	Gyro-Radius	170 km	636 km	896 km
4	Drift Speed	60 km/s	10 km/s	5 km/s
4	Gyro-Radius	120 km	280 km	280 km

Table 3A. Photoionization Rates

Reaction	Reaction Rate sec^{-1}	Reference
$H_2 + h\nu \rightarrow H^+ + H + e$	10^{-10}	Huebner & Giguere, 1980
$H_2 + h\nu \rightarrow H_2^+ + e$	5.9×10^{-10}	Huebner & Giguere, 1980
$H + h\nu \rightarrow H^+ + e$	8×10^{-10}	Huebner & Giguere, 1980
$N + h\nu \rightarrow N^+ + e$	2×10^{-9}	Huebner & Giguere, 1980
$N_2 + h\nu \rightarrow N_2^+ + e$	3.9×10^{-9}	Huebner & Giguere, 1980
$CH_4 + h\nu \rightarrow CH_4^+ + e$	6.5×10^{-9}	Huebner & Giguere, 1980

Table 3B. Electron Impact Ionization Rates

Reaction	Reaction Rate cm^3/s	Reference
$H + e \rightarrow H^+ + 2e$	5.13×10^{-9}	Lotz, 1966
$H + e^* \rightarrow H^+ + 2e$	3.1×10^{-8}	Lotz, 1966
$H_2 + e \rightarrow H^+ + H + 2e$	6.3×10^{-9}	Rapp & Englander-Golden, 1965

$H_2 + e^* \rightarrow H^+ + H + 2e$	$5.13x10^{-8}$	Rapp & Englander-Golden, 1965
$N_2 + e \rightarrow N_2^+ + 2e$	$1.02x10^{-8}$	Rapp & Englander-Golden, 1965
$N_2 + e^* \rightarrow N_2^+ + 2e$	$1.64x10^{-7}$	Rapp & Englander-Golden, 1965
$CH_4 + e \rightarrow CH_4^+ + 2e$	$2.33x10^{-8}$	Rapp & Englander-Golden, 1965
$CH_4 + e^* \rightarrow CH_4^+ + 2e$	$2.2x10^{-7}$	Rapp & Englander-Golden, 1965
$N + e \rightarrow N^+ + 2e$	$6.59x10^{-9}$	Lotz, 1966
$N + e^* \rightarrow N^+ + 2e$	$9x10^{-8}$	Lotz, 1966

Table 3C. Charge Exchange Reaction Rates

Reaction	Reaction Rate cm^3/s (225km/s)	Cross section $10^{-16}cm^2$ (260 eV/amu)	Reference
$H^+ + H \rightarrow H + H^+$	$5.0x10^{-8}$	22.0	Tawara 1985; Newman et al., 1982
$H^+ + H_2 \rightarrow H + H_2^+$	$17.x10^{-10}$	0.77	Tawara 1985; Tawara, 1978
$H_2^+ + H_2 \rightarrow H_2 + H_2^+$	$6.6x10^{-9}$	2.9	Massey & Gilbody, 1974
$H_2^+ + H \rightarrow H_2 + H^+$	$2.25x10^{-8}$	10.0	Estimate
$H^+ + N \rightarrow H + N^+$ [1]	10^{-8}	4.4	Basu et al., 1987
$H^+ + N_2 \rightarrow H + N_2^+$	$2.3x10^{-9}$	1.02	Rees, 1989; Rudd et al., 1985
$H^+ + N_2 \rightarrow H^+ + N_2^+$ [5]	$4.5x10^{-10}$	0.2	Basu et al., 1987
$H^+ + CH_4 \rightarrow H + CH_4^+$	$7x10^{-8}$	31.0	Rudd et al., 1985; Koopman, 1968
$H_2^+ + N \rightarrow H_2 + N^+$	$2.25x10^{-8}$	10.0	Estimate
$H_2^+ + N_2 \rightarrow H_2 + N_2^+$	$4.5x10^{-9}$	2.0	Estimate
$H_2^+ + CH_4 \rightarrow H_2 + CH_4^+$	$4.8x10^{-8}$	21.	Koopman, 1968
$N^+ + CH_4 \rightarrow N + CH_4^+$	$9.4x10^{-10}$	0.42	Albritton, 1978
$N_2^+ + CH_4 \rightarrow N_2 + CH_4^+$ [2]	10^{-9}	0.44	Albritton, 1978
$N^+ + N \rightarrow N + N^+$ [3]	$1.4x10^{-8}$	6.2	Lo et al., 1971
$N^+ + N_2 \rightarrow N + N_2^+$	$1.7x10^{-8}$	7.5	Phelps, 1991
$N^+ + H \rightarrow N + H^+$ [4]	$1.7x10^{-8}$	7.5	Tarawa 1985; Phaneuf et al., 1978
$N^+ + H_2 \rightarrow N + H_2^+$ [4]	$8.4x10^{-9}$	3.7	Tarawa 1985 ; Phaneuf et al., 1978
$N_2^+ + N \rightarrow N_2 + N^+$	10^{-11}	0.0044	Albritton, 1978
$N_2^+ + H \rightarrow N_2 + H^+$	$4.5x10^{-8}$	20	Estimate
$N_2^+ + N_2 \rightarrow N_2 + N_2^+$	$0.7x10^{-8}$	3.	Estimate
$CH_4^+ + H \rightarrow CH_4 + H^+$	$0.4x10^{-8}$	2	Estimate

$CH_4^+ + H_2 \rightarrow CH_4 + H_2^+$	0.2×10^{-8}	1.	Estimate
$CH_4^+ + N \rightarrow CH_4 + N^+$	0.1×10^{-8}	0.5	estimate
$CH_4^+ + N_2 \rightarrow CH_4 + N_2^+$	0.1×10^{-8}	0.5	Estimate
$CH_4^+ + CH_4 \rightarrow CH_5^+ + CH_3$	1.15×10^{-9}	0.57	Huntress, 1977

1. Used $H^+ + O \rightarrow H + O^+$ reaction at $E_p = 1$ keV
2. Actual end products are CH_3^+ & CH_2^+
3. Used $N^+ + O \rightarrow N + O^+$ reaction at E = 40 keV
4. Used cross-section at $E_{N+} = 10$ keV
5. Used cross-section at $E_p = 1$ keV

Figure Captions

Figure 1. Rendition of the interaction of Titan's upper atmosphere with Saturn's magnetosphere as observed by the Voyager 1 spacecraft during its close encounter with Titan as originally proposed by Hartle et al. (1982). The figure shows the alignment of the PLS sensors A, B, C and D relative to Titan and the upstream flow. The figure also shows the spacecraft trajectory and the ion spectra recorded by the plasma instrument and numbered 1 to 8.

Figure 2. This figure shows the ion spectra recorded by the PLS instrument for those outside the wake region. This figure shows the response of the instrument to the ambient plasma, its interaction with Titan and the presence of pickup ions.

Figure 3. Model of Titan's exosphere, which includes H, H_2, N^*, CH_4 and N_2, that was used for our mass loading calculations. See text for details.

Figure 4. This figure shows the effects of mass loading for various impact parameters of the flow relative to Titan's center. See text for details.

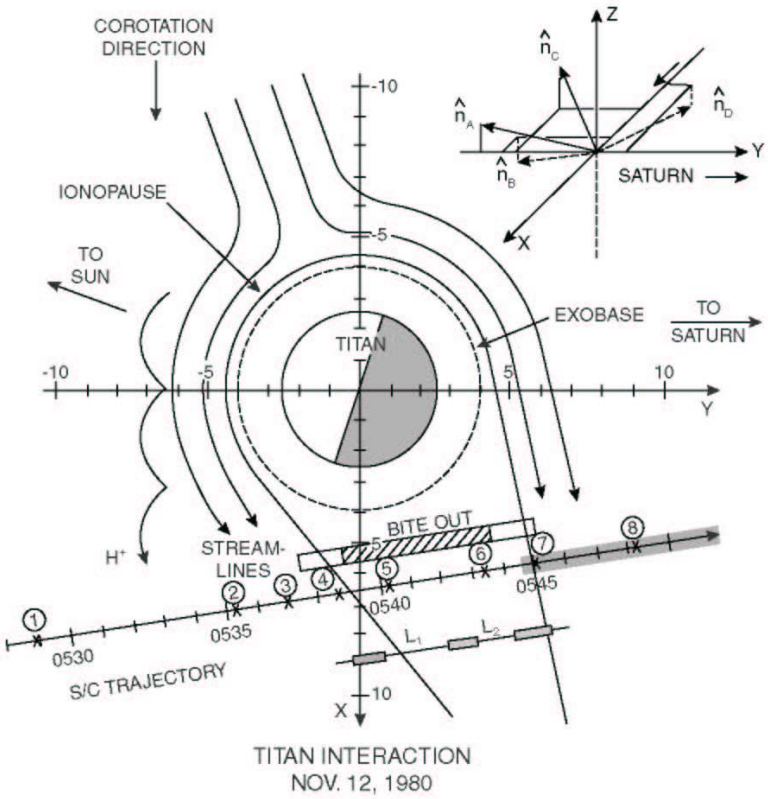

TITAN INTERACTION
NOV. 12, 1980

Figure1.

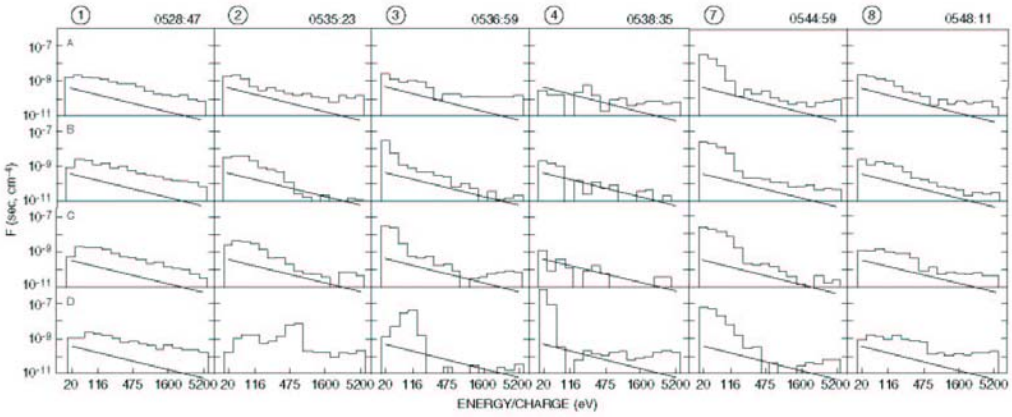
① 0528:47
② 0535:23
③ 0536:59
④ 0538:35
⑦ 0544:59
⑧ 0548:11
A
B
C
D
F (sec, cm⁻⁴)
20 116 475 1600 5200
ENERGY/CHARGE (eV)

Figure2.

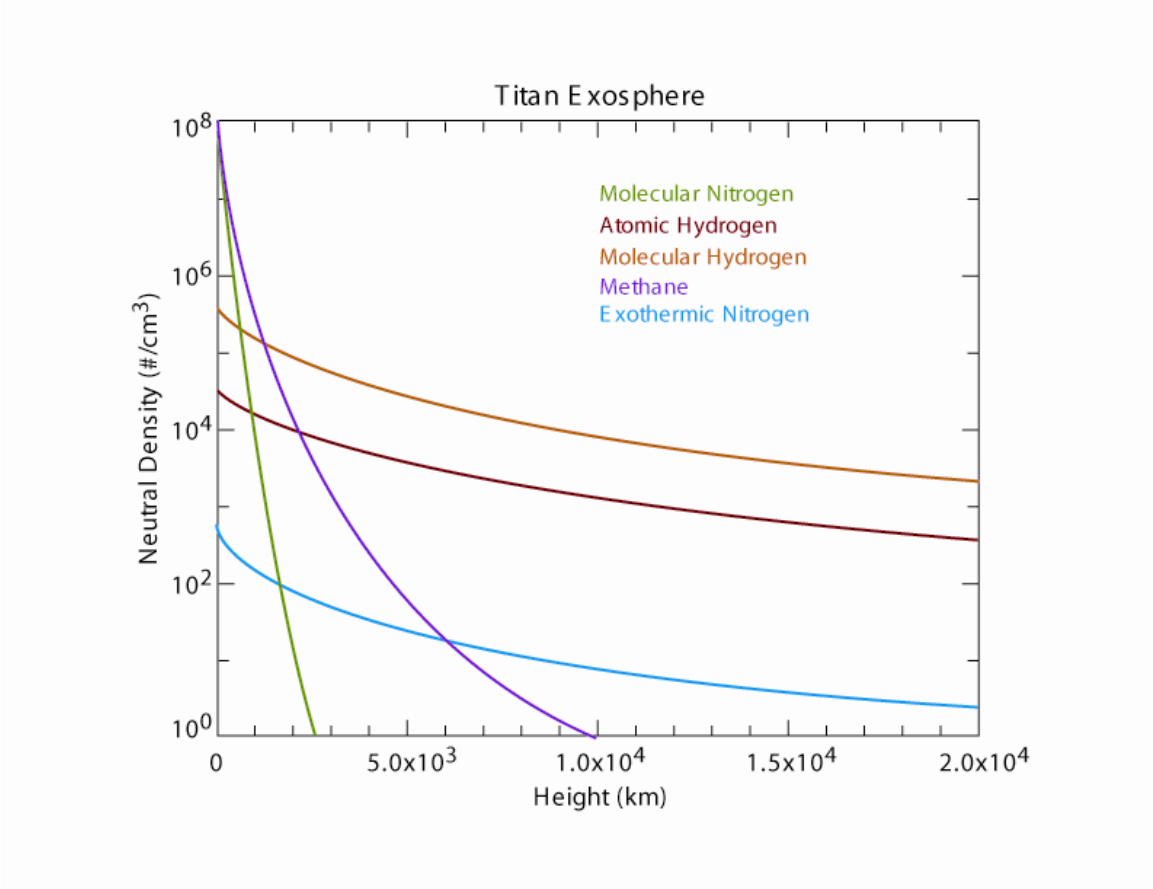
Titan Exosphere
Molecular Nitrogen
Atomic Hydrogen
Molecular Hydrogen
Methane
Exothermic Nitrogen
Neutral Density (#/cm3)
10^8
10^6
10^4
10^2
10^0
0
5.0x10^3
1.0x10^4
1.5x10^4
2.0x10^4
Height (km)

Figure 3.

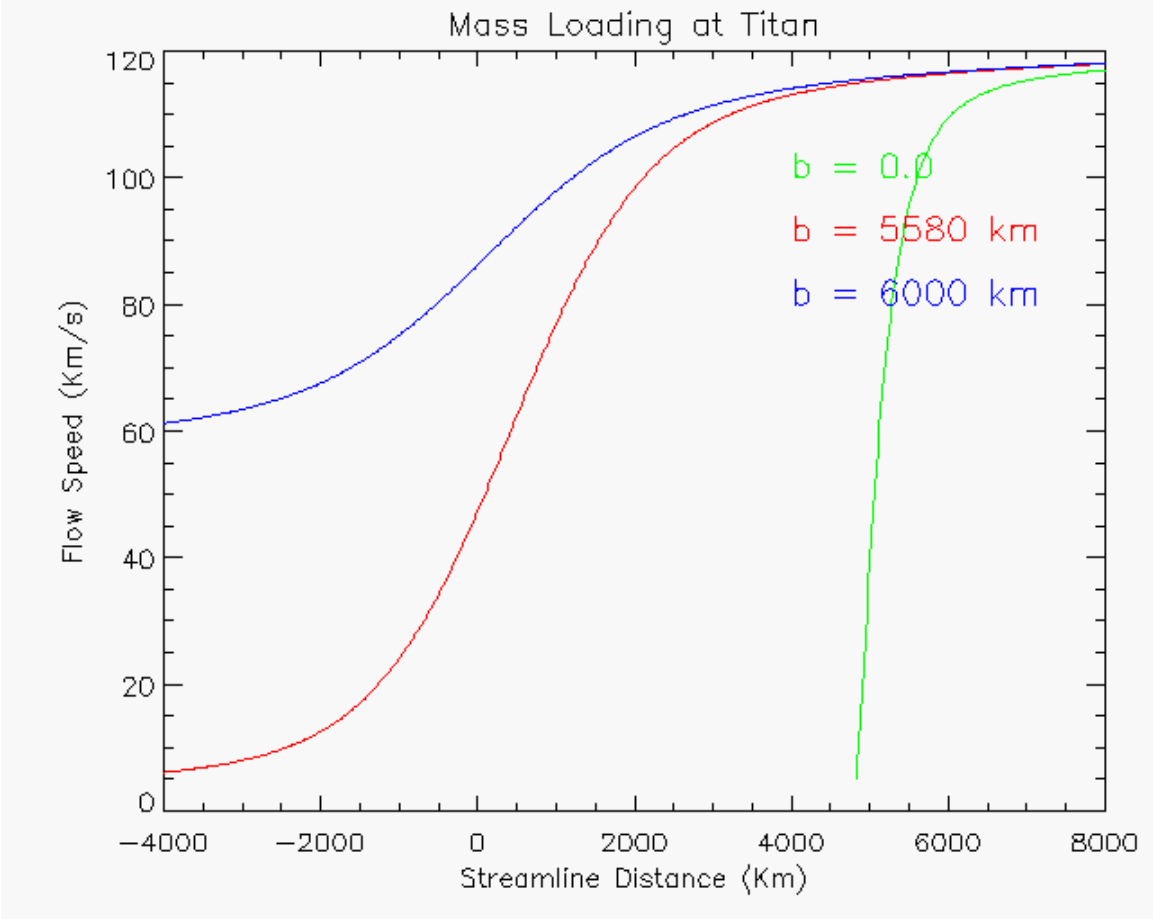
Mass Loading at Titan
b = 0.0
b = 5580 km
b = 6000 km
Flow Speed (Km/s)
Streamline Distance (Km)
120
100
80
60
40
20
0
−4000
−2000
0
2000
4000
6000
8000

Figure 4.